



## Treatment of Industrial Dye Effluent by Photo-Catalytic Process

### Using Modified Egyptian Bentonite

Sanaa M. Solyman\*, Hanan A. Ahmed

Egyptian Petroleum Research Institute (EPRI), Petrochemical Department, Nasr-City, Cairo, Egypt, PO Box 11727.



CrossMark

#### Abstract

Dyes are known to be harmful organic compounds for the environment since only a small amount of dyes can be hazardous. So, the treatment of industrial dye effluent using a commercial and effective catalyst is the study's main objective. The adsorptive and photo-catalytic activity of the Egyptian bentonite was improved by acid treatment, followed by incorporation of cerium dioxide on bentonite surface via simple precipitation method and then thermal treatment by calcination. The natural bentonite and the modified bentonite (B-CeO<sub>2</sub>) samples were characterized by XRD and TEM-EDX techniques. The removal% of dye was studied by changing the initiator, catalyst dosage, temperature, and solution pH in dark and visible light. The maximum dye removal (91%) was obtained in acidic solution (6.34, the normal pH of dye effluent) using 2 g/L catalyst dosage, 5 mM/L ammonium persulfate, 200 W lamp at 40 °C with constant stirring. The results indicated that the modified bentonite has high photo-catalytic activity in dye treatment due to a synergism between the effect of light, ammonium persulfate, CeO<sub>2</sub>, and exfoliated/delaminated bentonite.

**Keywords:** Modified bentonite, Cerium dioxide, Dye removal, Characterization.

#### 1. Introduction

The growing amount of contaminants in water has motivated the search for more promising adsorbents at low cost, especially for dyes present in the textile industry wastewater. Different textile dyes are mainly synthetic and feature complex molecular aromatic structures that make them more stable and difficult to breakdown. Dyes are categorized as anionic dyes (acid, direct, and reactive), cationic dyes (basic), and nonionic dyes (disperse) [1]. In anionic and nonionic dyes, the chromospheres consist mainly of azo groups or forms of anthraquinone. Anthraquinone-based dyes are more resistant to degradation due to their fused aromatic structures. The effluent produced by the textile industry is highly colored due to the residual dye that is not attached to the fabric. It cannot be ignored that these synthetic dyes are predominantly toxic, carcinogenic, and mutagenic.

They are also detrimental to the environment due to their bonds which are undegradable easily with the potential for persistence and accumulation in the environment. Clays are known to be cost-effective adsorbents [2]. The most frequent and successful type of clay used in wastewater treatment is bentonite. Bentonite is often impure and consists primarily of montmorillonite (MMT); however, some may consist of eidelite, saponite, hectorite, and nontronite may be present. The montmorillonite crystal consists of a sheet of octahedral alumina between two sheets of tetrahedral silica [3]. The chemical structure of clay makes it capable of attracting and holding cations and organic molecules having charges. The cation exchange capacity (CEC) depends on the form of clay and it's the highest one in montmorillonite clay. Different modified clays, such as organo-bentonite, pillared clay, acid treatment clay, thermal and microwave treatment, and other approaches were

\*Corresponding author e-mail: [sanaa8763@hotmail.com](mailto:sanaa8763@hotmail.com)

Receive Date: 23 August 2021, Revise Date: 06 October 2021, Accept Date: 12 October 2021 DOI: 10.21608/EJCHEM.2021.92237.4376

©2022 National Information and Documentation Center (NIDOC)

discussed by Leodopoulos et al. [4]. The efficiency of natural bentonite (MMT) in the removal of diazo dye was improved by acid activation (AA), thermal activation (TA), and acid-thermal activation (ATA) [2]. Acid activation of bentonite improves its adsorption efficiency due to 1) the exchangeable cations present in interlayer spaces being replaced by protons ( $H^+$ ) that penetrate the clay layers, 2) increasing the number of active sites, the specific surface area, acidity, and porosity, and 3) eliminating the mineral impurities with the partial dissolution of the external layers [2]. Thermal activation of bentonite (calcination) results in 1) a more porous material because of the loss of sorbed moisture, resulting in more adsorption sites, 2) delamination of the aluminosilicate layers increase the space available between the silicate layers and so the surface area, and 3) affects the textural properties and influences bentonite dispersibility in water [2]. Mustapha et al. studied the application of  $TiO_2$  and  $ZnO$  nanoparticles immobilized on clay in wastewater treatment [3]. They concluded that  $TiO_2$  and  $ZnO$  anchored on clay were promising for wastewater remediation and explored using nanotechnology. Photo-catalytic wastewater treatment, particularly in visible light, with promising results, is a good objective. Cano-Franco et al. studied the effect of  $CeO_2$  content in morphology and optoelectronic properties of  $TiO_2$ - $CeO_2$  nanoparticles in visible light degradation of methylene blue [5]. They found that  $TiO_2$ - $CeO_2$  nanoparticles are suitable for high photo-catalytic activity applications under visible light due to the effect of  $CeO_2$  content.

The main objective of our article is to prepare a commercial and promising photo-catalyst that can be used in the visible light range for the treatment of dyes in the effluent of the textile industry wastewater. Bentonite (B) was activated by acid treatment, cerium dioxide incorporation on the acid-treated bentonite surface in the presence of CTAB then activated thermally by calcination. The natural bentonite (B) and the modified bentonite (B- $CeO_2$ ) samples were characterized by XRD and TEM-EDX techniques. Additionally, the photo-catalytic activity of the produced catalyst (B- $CeO_2$ ) was studied in dye removal from textile industrial wastewater. Different variables including time, initiator, temperature, pH, dark, and visible light were studied.

## 2. Experimental Part

### 2.1. Materials used in the photo-catalytic treatment

The materials used in the experimental study were acetic acid ( $CH_3COOH$ ), cetyl trimethyl ammonium bromide (CTAB), cerium nitrate hexahydrate ( $Ce(NO_3)_3 \cdot 6H_2O$ ), and sodium hydroxide (NaOH). All the mentioned chemicals were obtained from Sigma-Aldrich, Germany. The dye effluent was obtained from the Tenth of Ramadan Factories for dyeing, printing, and processing. Table 1 shows the Physico-chemical properties of the dye effluent.

### 2.2. Catalyst preparation

Firstly, 10 g of natural bentonite (B) was treated with 100 mL of acetic acid by stirring overnight then

Table 1. The Physico-chemical properties of the effluent sample

Experiments analysis	Dye effluent sample
Temperature °C	25
pH	6.34
Suspended soiled (mg/L)	800
Phosphate (mg/L)	25
Nitrate (mg/L)	100
Sulfide (mg/L)	10
Colour	Pink

filtered and dried overnight at 110 °C [2]. Secondly, 1 g CTAB was dissolved in 100 mL of deionized (DI) water under stirring then 0.315 g of cerium nitrate hexahydrate was added to the obtained solution with stirring at room temperature [6]. When the solution became homogeneous, 5 g of acid-treated bentonite was added with constant stirring for 1 h. Thirdly, the precipitant NaOH solution (0.3 M) dropped wisely added until pH 12 was achieved and continued stirring for another 2 h [7, 8]. The obtained mixture was left for aging overnight after which the modified bentonite with cerium dioxide was filtered from the mixture, washed several times with DI water to get rid of the residual CTAB, dried overnight at 60 °C, and calcined for 4 h at 550 °C in air. The modified catalyst sample was named B- $CeO_2$ .

### 2.3. Characterization of catalyst

The natural bentonite (B) and the modified bentonite (B- $CeO_2$ ) samples were characterized using

two techniques. X-ray diffraction (XRD) was used to investigate the crystalline phases of the samples. The XRD patterns were recorded with a Pan Analytical Model X Pert Pro, which was equipped with CuK radiation ( $\lambda = 0.1542$  nm), Ni-filter, and general area detector. The diffractograms were recorded in the  $2\theta$  range of  $4-74^\circ$  with a step size of  $0.02^\circ$  and a step time of 0.605 min. Microscopy images and elemental analysis were obtained by transmission electron microscopy (TEM) and energy-dispersive X-ray spectroscopy (EDX) obtained by a JEOL JEM-1230 operating at 120 kV attached to a CCD camera and a Zeiss ULTRA Plus field-emission equipped with a Schottky cathode.

#### 2.4. Photo-catalytic treatment of dye effluent

The performance of B-CeO<sub>2</sub> was tested in the treatment of the effluent textile industry wastewater (Figure 1a) at different variables: catalyst weight (0.063 g and 0.1 g), in dark and in light (100 W and 200 W lamps of visible light used at home), at different temperatures (25, 40 and 60 °C), different pHs (2, 6.34 and 9), and different initiators (FeSO<sub>4</sub>, (NH<sub>4</sub>)<sub>2</sub>S<sub>2</sub>O<sub>8</sub>, and TiSO<sub>4</sub>), with taking samples at different time intervals. The pH was adjusted by using NaOH and HCl solutions. A blank test was processed firstly by adding 0.063 g of the catalyst B-CeO<sub>2</sub> to 50 mL of dye wastewater without adding initiator, at room temperature, natural pH of the effluent (6.34), and in the dark atmosphere. The reaction mixture was stirred and samples (10 mL) from the treated effluent were taken each 10 min, filtered, and analyzed. The concentration of dye was monitored by HACH spectrophotometer DR/2000 at wavelength  $\sim 450$  nm. The test was repeated by changing the variables and taking samples at different time intervals each 1 h. The dye removal% = [(The absorbance of the blank sample – the absorbance of the treated sample) / the absorbance of the blank sample] X 100. Figure 1b shows the photocell used in the dye treatment. It contains a magnetic stirrer, fan for cooling, and lamps fixed with 30 cm distance from the waste solution which was inserted in a beaker with the reactants and magnet.

### Results and Discussion

2.5. XRD and TEM-EDX patterns and the TEM micrographs of B and B-CeO<sub>2</sub> samples as well as the EDX results of B-CeO<sub>2</sub> are represented in **figure 2(a-d)**. From the XRD patterns, the characteristic peaks

of bentonite (Ref. code 00-003-0019) appear at 2-theta values of  $6.96^\circ$ , several peaks at  $\sim 20^\circ$ ,  $26.65^\circ$ , and others as shown in **figure 2a**.



Figure 1 (a) The pink color of the dye effluent wastewater and (b) The photocell used in the dye treatment experiment.

The intensity of the signals of bentonite (B) is decreased after modification in sample B-CeO<sub>2</sub> without appearing any bands for CeO<sub>2</sub> [9]. These findings are mainly due to a reduction in bentonite particle size (delamination) and/or intercalation of CeO<sub>2</sub> as a very fine nano-particle with the bentonite surface [10]. These observations are confirmed by TEM-EDX analysis. The TEM micrographs of B and B-CeO<sub>2</sub> samples (**Figure 2 (b, c)**) show the dispersion of CeO<sub>2</sub> on bentonite surface and confirm the delamination of bentonite after modification. EDX results (**Figure 2d**) confirm the presence of Ce, O, Si, and Al elements in the composition of the prepared B-CeO<sub>2</sub> catalyst. The mentioned elements represent all the modified catalyst elements, therefore, confirming its successful modification [9].

#### 2.6. Photo-catalytic treatment of dye effluent

The performance of bentonite was improved by its acidic treatment using acetic acid followed by the incorporation of CeO<sub>2</sub> into bentonite platelets (B-CeO<sub>2</sub>) then thermal activation by calcination. As previously published, mild acid treatment conditions increased the adsorption properties of clays by increasing the number of active sites, specific surface area, acidity, and porosity [4].

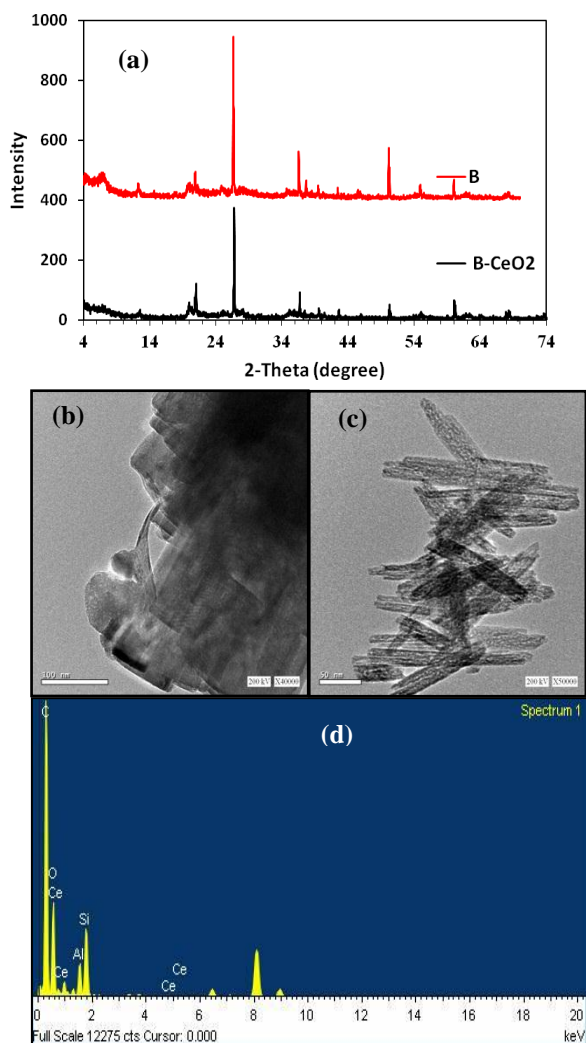


Figure 2 (a) XRD of bentonite (B) and modified bentonite (B-CeO<sub>2</sub>), (b) TEM of bentonite (B), (c) TEM of modified bentonite (B-CeO<sub>2</sub>), and (d) EDX of B-CeO<sub>2</sub>.

The authors also concluded that acid treatment resulted in the disaggregation and delamination of clay platelets which are responsible for increasing the structural properties. This disaggregation and delamination are observed in the TEM micrographs of our work (**Figure 2(b, c)**) mostly indicating new structural properties. We studied the dye removal% at different variables: in dark and visible light, different initiators, different pHs, and temperatures with constant stirring as will be shown in the following sections. The factors will be constant as catalyst concentration is 1.25 g/L, pH is 6.34, and ammonium persulfate concentration is 5 mM/L at room temperature with constant stirring while studying any of them.

### 2.6.1. Effect of B-CeO<sub>2</sub> catalyst in dark with/without the initiator on dye removal

The performance of B-CeO<sub>2</sub> (1.26 g/L) is measured as the removal% of dye effluent at different time intervals in dark with/without ammonium persulfate 5 mM/L as the initiator (**Figure 3**). Firstly, this Figure shows that the addition of the initiator enhances the removal% of dye in dark. Without initiator, a removal% of 11.2% was obtained after 20 min which was increased to 38.8% at 60 min then decreased to 30.3% at 120 min. When the reaction was repeated by the addition of the initiator at the same above conditions, the dye removal% was increased to 59.87% at 60 min and a maximum removal% of 64.5% was achieved after 180 min. This enhancement may be due to the synergism between the new structural properties of bentonite, the effect of the initiator, and the redox ability of CeO<sub>2</sub> incorporated on the bentonite surface.

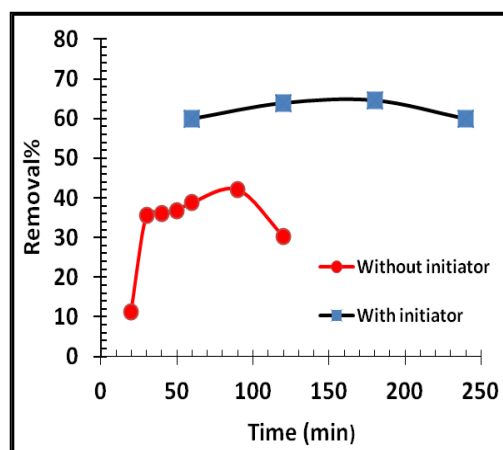


Figure 3 The effect of B-CeO<sub>2</sub> catalyst on dye removal% in dark with/without ammonium persulfate as initiator at room temperature and at different time intervals

The CeO<sub>2</sub> mostly activates the dissociation of ammonium persulfate creating free radicals by the oxidation-reduction reaction. These free radicals target the dye molecules and the degradation begins. For comparison, natural bentonite without modification (1.26 g/L) is tested using ammonium persulfate concentration (5 mM/L) in the dark, which gives dye removal% of 10% after 4 h. These results indicated that the modified bentonite (B-CeO<sub>2</sub>) produces new surface properties which resulted in an excellent improvement in dye treatment especially in the presence of the initiator.



### 2.6.2. The effect of visible light on dye treatment

Photo-activation results are shown in **figure 4** using the visible light lamps (100 W and 200 W) and taking samples with intervals of 1 h and compared with the results obtained in dark and by the addition of initiator.

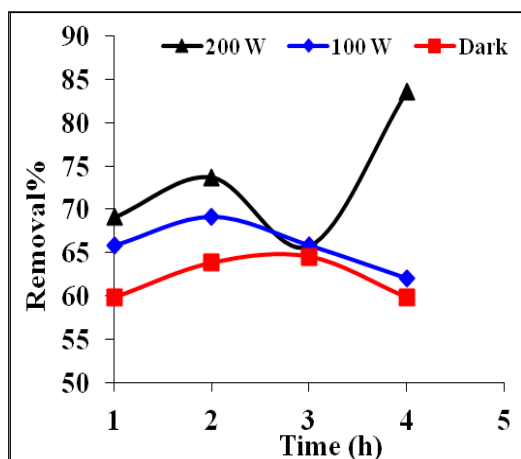


Figure 4 The effect of dark, 100 W, and 200 W lamps on the removal% of dye at different time intervals using 1.25 g/L catalyst concentration, 5 mM/L ammonium persulfate initiator with stirring at room temperature.

The comparison indicates firstly that after 1 h, the removal% increased from 59.87% in dark with the initiator to 65.8% and 69% using 100 W and 200 W lamps, respectively due to photo-activation as shown in **figure 4**. Secondly, after 2 h, the removal% still increases with/without light. Thirdly, the maximum removal% obtained in dark, 100 W, and 200 W were 64.5, 69, and 83.6% after 3, 2, and 4 h, respectively. According to the previous publications [4, 5],  $\text{CeO}_2$ -based systems have photo-catalytic activity in dye degradation in the visible spectrum range.  $\text{CeO}_2$  is known to have high redox properties (low reduction potential between  $\text{Ce}^{3+}$  and  $\text{Ce}^{4+}$ ) which are mostly activated by visible light [11] and create extra free radicals in presence of ammonium persulfate. These factors increased the degradation of dye molecules resulted in increasing the dye removal to 83.6% using the catalyst (1.26 g/L), initiator (5 mM/L), and the visible light (200 W lamp) at room temperature.

### 2.6.3. Effect of catalyst dosage

**Figure 5** demonstrates the influence of catalyst dosage (1.26 g/L and 2 g/L) on the dye removal% at the same abovementioned conditions using the 200 W lamp. The dye removal% was increased from 69%

to 86.2% after 1 h and the removal% was reached 83.6% after 4 h and 88.2% after 3 h using 1.26 g/L and 2 g/L catalyst concentration respectively. This enhancement is mostly due to increasing the number of active sites. This result may indicate that the rate of dye adsorption and desorption are nearly equal, and/or 2 g as a catalyst dosage is suitable to give good degradation.

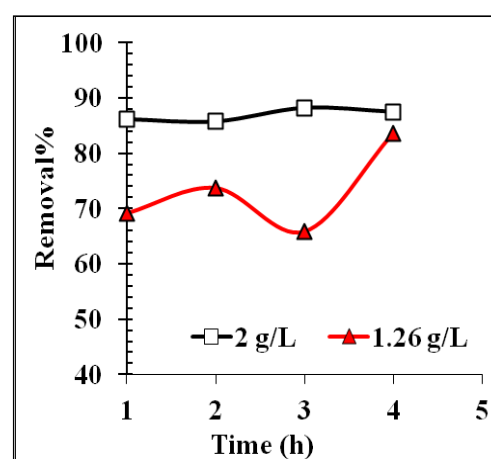


Figure 5 The effect of catalyst dosage on dye removal% at different time intervals using 5 mM/L ammonium persulfate as initiator, 200 W lamp with stirring at room temperature

### 2.6.4. Effect of different initiators

**Figure 6** shows the effect of different initiators ( $(\text{NH}_4)_2\text{S}_2\text{O}_8$ ,  $\text{FeSO}_4$ , and  $\text{TiSO}_4$  with 5 mM/L concentration on dye removal% using 200 W lamp, catalyst concentration of 2 g/L at pH 6.34 with stirring at room temperature. Previously, De Castro et al. studied the adsorption of MB (cationic dye) and  $\text{Cu}^{+2}$  on EMB at different conditions [12]. They found that the hydrated ionic radii of cations and anions and the ionic strength of different salts have an important role in the adsorption capacity for adsorbates. As a comparison, we have anionic dye in the present study so the adsorption capacity correlated with the values of hydrated ionic radii for cations  $\text{NH}_4^+$ ,  $\text{Fe}^{+2}$ , and  $\text{Ti}^{+2}$  which were found to be 1.25, 3, and 1.25 Å respectively. The order of removal capacity enhancement was  $\text{TiSO}_4 < \text{FeSO}_4 < (\text{NH}_4)_2\text{S}_2\text{O}_8$  as shown in figure 6. The smaller hydrated ionic radii of  $\text{Ti}^{+2}$  (1.25 Å) relative to  $\text{Fe}^{+2}$  (3 Å) make titanium cations are easier to attract to and surround the dye molecules and inhibit their adsorption on the catalyst active sites. So, the maximum removal% using  $\text{TiSO}_4$  and  $\text{FeSO}_4$  are 79.6

and 86.2 respectively after 2 h. Also,  $\text{Fe}^{+2}$  and  $\text{Ti}^{+2}$  are electron deficient cations and have a high ability to attract anionic dye molecules so, the removal% decreases after 2 h. As a result,  $(\text{NH}_4)_2\text{S}_2\text{O}_8$  has a better improvement effect and produces 85.5% and 88.2% removal% after 2 and 3 h, respectively. According to De Castro et al., the ionic strength of  $(\text{NH}_4)_2\text{S}_2\text{O}_8$ ,  $\text{FeSO}_4$ , and  $\text{TiSO}_4$  as salts are calculated using the following equation:  $I = 0.5 \sum \text{Ci} \cdot \text{Zi}^2$ , (I) is the ionic strength, (Ci) is the concentration, and (Zi) is the number of charges of cations or anions. The ionic strength values were found to be 0.02 M for all salt solutions used in our study which indicates that this factor is not effective. It can be concluded that the maximum removal% was 88.2% using ammonium persulfate due to a synergism between the effect of hydrated ionic radii, the created free radicals, the electron deficiency of cations ( $\text{Fe}^{+2}$  and  $\text{Ti}^{+2}$ ), and the effect of photo-catalytic activation.

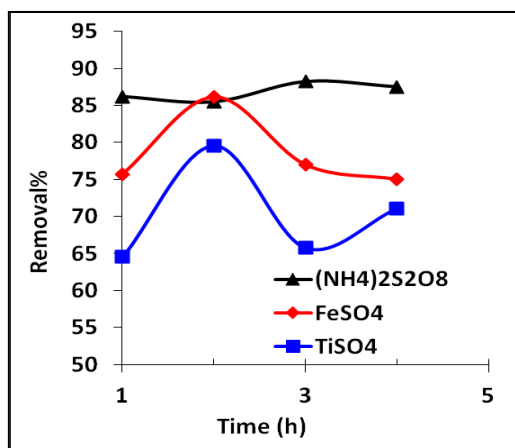


Figure 6 Effect of different initiators on the removal% of dye at different time intervals using 2 g/L catalyst, 5 mM/L initiator concentration, 200 W l

#### 2.6.5. Effect of pH change

Previous publications concluded that the solution pH plays an important role in controlling the surface charge of the adsorbent, the degree of ionization of the adsorbate in the solution as well as dissociation of various functional groups on the active sites of the adsorbent. In most cases, pH is termed as the 'master variable' [13].

Figure 7 shows the results of the experiments of the dye removal% that were obtained at pH values of 2, 6.34 (the normal value of dye effluent), and 9 under the optimum conditions studied above. This

figure shows that the removal% increases in acidic solutions (pH=2 and 6.34) but decreases in alkaline solution (pH=9). This confirms that the type of dye in wastewater effluent is an anionic dye type [14, 15]. The active sites of B-CeO<sub>2</sub> will have a positive charge in acidic solution which strongly increases the electrostatic interaction and enhance the uptake and the removal% of dye molecules [16]. On the other hand, in alkaline solution (at pH=9) the removal% decreased mostly because anionic dye molecules and OH<sup>-</sup> of alkaline solution compete on the catalyst adsorption sites. The highest removal% values are 90% after 2 h at pH=2, 88.2% after 3 h at pH= 6.34 and 57.2% after 4 h at pH=9 [16].

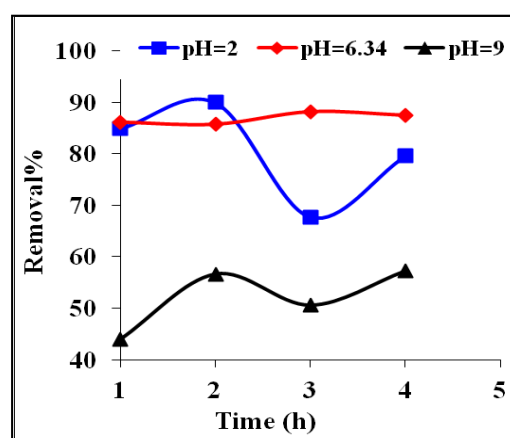


Figure 7 Effect of solution pH on dye removal% at different time intervals using 2 g/L catalyst concentration, 5 mM/L ammonium persulfate concentration, 200 W lamp with stirring at room temperature.

#### 2.6.6. Effect of temperature

Figure 8 demonstrates the influence of different temperatures (25, 40, and 60 °C) on the dye uptake from the wastewater effluent. The maximum removal% of the dye molecules was 88.2% at 25 °C after 3 h, 91% at 40 °C after 2 h, and 82.9% at 60 °C after 1 h. Temperature is known to increase the diffusion of adsorbate molecules through the outer surface and the inner pores of adsorbent particles [17]. As the temperature increased from 25 °C to 40 °C, the mobility and diffusion of the dye molecules through B-CeO<sub>2</sub> pores increased, so the maximum adsorption% increased but decreased at 60 °C mostly due to the desorption of dye molecules.

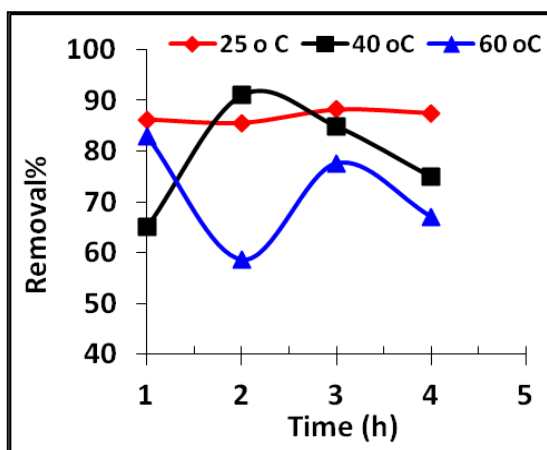


Figure 8 Effect of temperature on dye removal% at different time intervals using 2 g/L catalyst concentration, 5 mM/L ammonium persulphate concentration, and 200 W lamb with stirring.

### 3- Conclusion

The main objective of this study was the treatment of industrial dye effluent using a commercial and effective catalyst and light lamps (used at home). Egyptian bentonite was modified by acid treatment followed by the incorporation of cerium dioxide on the bentonite surface (by simple precipitation technique), and then its thermal treatment. The natural bentonite and the produced catalyst sample (B-CeO<sub>2</sub>) were characterized by XRD and TEM-EDX which confirm new structural properties. It was concluded that the removal% of dye molecules is the overall result of the adsorption, desorption, and degradation of dye molecules. The dye removal% increases in acidic pH waste solution but decreases in alkaline solution indicating that the dye type contained in the wastewater effluent is an anionic dye. The elevation of reaction temperature increased the adsorption and desorption process, so the dye treatment at room temperature was more favorable. Ammonium persulfate plays an important role in enhancing dye removal in dark and visible light. Synergism between the effect of visible light, cerium dioxide, and ammonium persulfate creates more free radicals and increased the removal%. The maximum removal% was 91% at the optimum conditions (pH 6.34, 40 °C, 2 g/L catalyst concentration, 200 W lamb, and 5mM/L ammonium persulfate concentration). This study reports a highly efficient and cost-effective photo-catalyst for dye pollutant removal.

### 5. Conflicts of interest

There is no conflict of interest

### 6. References

1. Mustafa T. Yagub, Tushar Kanti Sen, Sharmeen Afroze, H.M. Ang "Dye and its removal from aqueous solution by adsorption: A review" *Advances in Colloid and Interface Science* **209**, 172-184(2014).
2. Adeyemo, A.A., I.O. Adeoye, and O.S. Bello, Adsorption of dyes using different types of clay: a review. *Applied Water Science*, **7**(2), 543-568(2017).
3. Mustapha S., Ndamitso M. M., Abdulkareem A. S., Tijani J. O., Shuaib D. T., Ajala A. O., and Mohammed A. K., Application of TiO<sub>2</sub> and ZnO nanoparticles immobilized on clay in wastewater treatment: a review. *Applied Water Science*, **10**(1), 1-36(2020).
4. Leodopoulos, C., D. Doulia, and K. Gimouhopoulos, Adsorption of cationic dyes onto bentonite. *Separation & Purification Reviews*, **44**(1), 74-107(2015).
5. Cano-Franco, J.C. and Álvarez-Láinez M., Effect of CeO<sub>2</sub> content in morphology and optoelectronic properties of TiO<sub>2</sub>-CeO<sub>2</sub> nanoparticles in visible light organic degradation. *Materials Science in Semiconductor Processing*, **90**, 190-197(2019).
6. Fadzil N.A.M., Rahim M.H.A., and Maniam G.P., Room Temperature Synthesis of Ceria by the Assisted of Cationic Surfactant and Aging Time. *Malays. J. Anal. Sci*, **22**, 404-415(2018).
7. Chelliah M., Rayappan J. B. B., and Krishnan U. M., Synthesis and characterization of cerium oxide nanoparticles by hydroxide mediated approach. *J. Appl. Sci*, **12**(16), 1734-1737(2012).
8. Nyoka M., Choonara Y. E., Kumar P., Kondiah P. P. D., and Pillay V., Synthesis of Cerium Oxide Nanoparticles Using Various Methods: Implications for Biomedical Applications. *Nanomaterials*, **10**(2), 242(2020).
9. Gorobinskii L.V., Yurkov G.Y., and Baranov D.A., Production of high porosity nanoparticles of cerium oxide in clay. *Microporous and mesoporous materials*, **100**(1-3),134-138(2007).
10. Wang Q., *Anodic electrochemical synthesis and characterization of nanocrystalline cerium oxide and cerium oxide/montmorillonite*

- nanocomposites*, Dissertation Abstracts International, 64-12B. (2003).
11. Singh, S. and Lo S.-L., Single-phase cerium oxide nanospheres: an efficient photocatalyst for the abatement of rhodamine B dye. *Environmental Science and Pollution Research*, **25**(7), 6532-6544(2018).
  12. De Castro M. L. F. A., Abad M. L. B., Genuino D. A. D., Abarca R. R. M., Paoprasert P., and De Luna M. D. G., Adsorption of methylene blue dye and Cu (II) ions on EDTA-modified bentonite: isotherm, kinetic and thermodynamic studies. *Sustainable Environment Research*, **28**(5), 197-205(2018).
  13. Banerjee, S. and Chattopadhyaya M., Adsorption characteristics for the removal of a toxic dye, tartrazine from aqueous solutions by a low cost agricultural by-product. *Arabian Journal of Chemistry*, **10**, S1629-S1638 (2017).
  14. Bellir K., Bencheikh-Lehocine M., Meniai A-H., *Removal of methylene blue from aqueous solutions using an acid activated Algerian bentonite: equilibrium and kinetic studies*. Int Renew Energy Congr, 360-367(2010).
  15. Silva M. M. F., Oliveira M. M., Avelino M. C., Fonseca M. G., Almeida R. K. S., and Silva Filho E. C., Adsorption of an industrial anionic dye by modified-KSF-montmorillonite: Evaluation of the kinetic, thermodynamic and equilibrium data, *Chemical engineering journal*, **203**, 259-268(2012).
  16. Özcan, A.S., Erdem B., and Özcan A., Adsorption of Acid Blue 193 from aqueous solutions onto Na-bentonite and DTMA-bentonite, *Journal of colloid and Interface science*, **280**(1), 44-54(2004).
  17. Patel, H. and R. T. Vashi, *Characterization and treatment of textile wastewater*. Elsevier , (2015).